Draft version May 6, 2025
Typeset using LaTeX **twocolumn** style in AASTeX7

Stellar Structure Report

Myles Pope[1]

[1] *Johns Hopkins University*

ABSTRACT

In this report, I give the details and results of a simple stellar model. I report on the calculation of the structure of a 1.2 $M_\odot$ star, tracing the pressure, radius, luminosity, and temperature throughout the stellar interior. A comparison is done of the model to the industry standard stellar structure and evolution code, MESA. I found that while the model could accurately reproduce the deep internal conditions of the star, it could only produce the most commonly measured observable surface properties by ≈30%.

1. INTRODUCTION

The detailed theory of how stars function internally has been pondered and studied for centuries. Following the discoveries of nuclear energy in the early 20th century, prolific theorists like A. S. Eddington (1920) started to postulate that stars gained their energy through nuclear fusion, and the study of stellar interiors got off to an explosive start. In this report, I aim to implement and code a simple model of stellar structure, in the hopes of providing a program that can provide solutions of some of the fundamental properties of intermediate mass zero age main sequence (ZAMS) stars.

2. THEORY

2.1. *Internal assumptions*

This model was directly adapted from C. J. Hansen et al. (2004). For this model, the star is taken as a spherically symmetric object in hydrostatic equilibrium and local thermodynamical equilibrium. These assumptions work well for the internal structure of a zero-age main sequence (ZAMS) star, given that the optical depth is much greater than one, and are the base that allows our differential equations to hold. Once the optical depth drops below one, the mean free path of the photons becomes sufficiently large, and our assumptions of local thermodynamic equilibrium break. Some major confounding factors that this model does not account for are the effects of rotation, oscillations and magnetic fields. I assume that the star is very slowly rotating, such that it does not affect the internal structure, and that any pulsations are regular and have low enough amplitude to averaged out over time to create a quasi-static object. For intermediate mass ZAMS stars, M≈0.8-5 $M_\odot$, these approximations aren't horribly inaccurate. Magnetic fields likely do play a large role in the structure of most stars, but the complex study of their effects is outside of the scope of this model.

2.2. *Opacity Tables*

I used the opacity tables from the OPAL database M. Asplund et al. (2005) for this project. The database contains grids of opacities calculated for stars of different compositions. A linear interpolation function as a part of scipy's library, **scipy.interpolate.RegularGridInterpolator** P. Virtanen et al. (2020), was used on the grid to get a denser output that could be used for any calculation.

2.3. *Structure Differential Equations*

The equations that describe how to the pressure, radius, luminosity, and temperature change with the Lagrangian mass coordinate are as follows:

$$\frac{dP}{d\mathcal{M}_r} = -\frac{G\mathcal{M}_r}{4\pi r^4} \tag{1}$$

$$\frac{dr}{d\mathcal{M}_r} = \frac{1}{4\pi r^2 \rho} \tag{2}$$

$$\frac{d\mathcal{L}_r}{d\mathcal{M}_r} = \varepsilon \tag{3}$$

$$\frac{dT}{d\mathcal{M}_r} = -\frac{G\mathcal{M}_r T}{4\pi r^4 P}\nabla \tag{4}$$

Where P, r, $\mathcal{L}_r$, and T are the pressure, radius, luminosity, and temperature, respectively. G is simply the Netownian gravitational constant, and ∇ is the differential temperature gradient, which depends on the method of energy transport with the annular region.

Email: mpope7@jh.edu

I used Schwarzschild's criteria to determine the method of energy transport of a region, which compares the radiative ∇,

$$\nabla_{\rm rad} = \left(\frac{d\ln T}{d\ln P}\right)_{\rm rad} = \frac{3}{16\pi acG}\frac{P\kappa}{T^4}\frac{\mathcal{L}_r}{\mathcal{M}_r} \tag{5}$$

Where κ is the rosseland mean opacity, a is the blackbody energy constant, G is the Newtonian gravitational constant, and c is the speed of light in a vacuum, to the adiabatic ∇

$$\nabla_{\rm ad} = \frac{1-\Gamma}{\Gamma} = 0.4 \tag{6}$$

where Γ is the third adiabatic exponent, taken as 5/3 for a monoatomic ideal gas.

The criteria states that if a region has a temperature gradient too high to be sustained by radiation, it will be convective. This is highlighted by the equation below for convective regions:

$$\nabla = \nabla_{\rm rad} \quad \text{if} \quad \nabla_{\rm rad} < \nabla_{\rm ad} \tag{7}$$
$$\tag{8}$$

and this equation for radiative regions:

$$\nabla = \nabla_{\rm ad} \quad \text{if} \quad \nabla_{\rm rad} > \nabla_{\rm ad} \tag{9}$$
$$\tag{10}$$

2.4. *Energy generation*

At the ZAMS, for low to intermediate mass stars, the vast majority of energy generation comes from the nuclear fusion of hydrogen into helium. There are 2 paths with which stars can fuse hydrogen, the pp-chain and the CNO cycle. The pp-chain takes 4 protons and fuses them into 1 alpha particle, giving off electron neutrinos and positrons in the process. The CNO cycle uses carbon, nitrogen and oxygen atoms to fuse with protons, creating alpha particles and some lighter metals. See C. J. Hansen et al. (2004) chapter 6 for exact reaction sequences and products. The equations used to calculate the rate of energy generation for the pp-chain depends on a self shielding factor f_{11} and a correction factor ψ that ranges from 1 to 2 in order to account for the different intermediate branches the pp-chain can take. The equations from R. Kippenhahn et al. (2012) are as follows:

$$f_{11} = \exp\left(5.92\times10^{-3}\left(\frac{\rho}{T_7^3}\right)^{1/2}\right) \tag{11}$$
$$g_{11} = 1 + 3.82T_9 + 1.51T_9^2 + 0.144T_9^3 - 0.0114T_9^4 \tag{12}$$
$$\psi = 1.2 \tag{13}$$
$$\epsilon_{pp} = 2.57\times10^4 \times g_{11}\psi\ f_{11}X^2\rho\ T_9^{-2/3} \tag{14}$$
$$\times \exp\left(-3.381\,T_9^{-1/3}\right) \tag{15}$$
$$\tag{16}$$

The CNO cycle equations are similar, with the main defining feature being that there is only one sequence of reactions, and that the rate now depends on the metallicity Z.

$$g_{14} = 1 - 2\,T_9 + 3.41\,T_9^2 - 2.43\,T_9^3 \tag{17}$$
$$\epsilon_{CNO} = 8.24\times10^{25} g_{14} XZ\rho \times T_9^{-2/3} \tag{18}$$
$$\times \exp\left(-15.231\,T_9^{-1/3} - \left(\frac{T_9}{0.8}\right)^2\right) \tag{19}$$

2.5. *Core conditions*

The model required initial core conditions and final surface conditions to be solved. I took our core conditions as the values of a small, spherical region of mass $m_{\rm small}$ = M $\times10^{-5}$, where M is the total mass of the star. The initial core values are listed immediately below. A note of caution on the variables, the core values, designated with subscript core, are NOT equal to the central values, which are taken at the very center of the star, m = 0, and designated with subscript c.

$$r_{\rm core} = \left(\frac{3m_{\rm small}}{4\pi\rho_c}\right)^{1/3} \tag{20}$$
$$P_{\rm core} = P_c - \frac{2\pi}{3}G\rho_c^2 r^2 \tag{21}$$
$$l_{\rm core} = \epsilon_c\, m_{\rm small} \tag{22}$$

The core temperature depended on the energy transport mechanism in the core, and is as follows, using the same variables in the previous section describing the radiative temperature gradient:

$$Radiative: T_{\rm core} = T_c - \frac{\epsilon_c^2\,\rho_c^2\,\kappa\,r^2}{8\,a\,c\,T_c^3} \tag{23}$$
$$Convective: T_{\rm core} = T_c - \frac{2\pi}{3}\frac{G\,\nabla_{\rm ad}\,\rho_c^2\,T_c\,r^2}{P_c} \tag{24}$$

2.6. *Surface conditions*

As for the surface conditions, I used a simple photospheric model, assuming that the radius and luminosity

were the total stellar radius and luminosity, and temperature was the effective blackbody temperature of an object with luminosity L at optical depth $\tau = 2/3$. The pressure is taken as a gray atmosphere approximation R. Kippenhahn et al. (2012), with $\kappa = 0.6$.

$$l_{\text{surf}} = L \tag{25}$$

$$r_{\text{surf}} = R \tag{26}$$

$$T_{\text{eff}} = \left(\frac{L}{4\pi R^2 \sigma_{\text{SB}}} \right)^{1/4} \tag{27}$$

$$P_{\text{surf}} = \frac{2}{3} \frac{GM}{R^2 \kappa} \tag{28}$$

3. NUMERICAL METHODS

3.1. *Shooting Method*

This program takes the differential equations laid out in Section 2.2, and integrates them over the entire mass of the star to find the individual parameters at each mass point. The method used to solve these equations is a shooting function, similar to the one outlined in W. H. Press et al. (2007) Chapter 18. The method involves solving the ODE system twice. One integration is bound from the surface of the star, taken as m=M, to a desired midpoint, and the other is bound from the core of the star, taken as $m = M \times 10^{-5}$, to that same midpoint. The initial values for each integral are outlined in sections 2.4 and 2.5. Each integral is numerically solved using **scipy.solve.ivp** function, with an explicit Runge-Kutta (RK45) method J. Dormand & P. Prince (1980). Initially, the ODE system appeared to be too stiff to solve with RK45, but integrating over a linearly spaced mass grid with 10000 points significantly improved the numerical stability. Other methods specifically designed for stiff systems were tried, namely scipy's backward's differentiation (BDF) and implicit Runge Kutta methods (Radau), but neither were as accurate as RK45.

3.2. *Optimization for Convergence*

After the initial shooting function was performed, a minimization routine was run on the parameters from both integrations at the midpoint. The residuals of the shooting function were calculated by taking the square of difference of the two integrations at the midpoint, which was then scaled to the bounds which was simply the difference between the surface and core boundary values.

After calculating the residuals, they were loaded into **scipy.minimize**, and a limited memory Broyden–Fletcher–Goldfarb–Shanno (L-BFGS) algorithm R. H. Byrd et al. (1995) is used to minimize the residuals and provide a new initial guess for the shooting function. The algorithm is a Quasi-Newtonian method that uses an inverse Hessian matrix for minimization, and is optimized for memory usage. A least squares approach was initially attempted, but ultimately performed much worse at minimizing the residuals. The optimized values are then used as the new starting conditions for the shooting solver, and the final results give the closest converged solution.

4. RESULTS

This model was used to calculate the internal structure of a 1.2 $M_\odot$ star with solar composition (X=0.7, Y=0.28, Z=0.02). The initial guesses are listed in Table 1, and were generated using a helper function, which used homology relationships to estimate the luminosity and radius based off the mass, and a modified constant density approximation for the central temperature and pressure, scaled to match the solar values for a 1 $M_\odot$ star.

Pc	$1.4791 * 10^{17}\ dyne\ cm^{-1}$
R	$7.6242 * 10^{10}\ cm$
L	$7.2423 * 10^{33}\ erg\ s^{-1}$
Tc	$1.5796 * 10^{7}\ K$

Table 1. Initial Integration Guesses

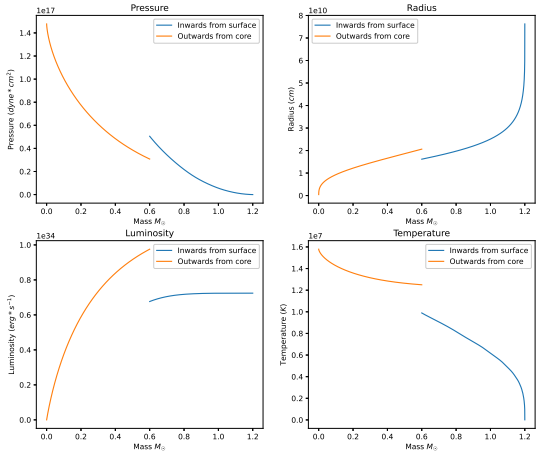

Figure 1. Initial Unconverged Integrations

The integrations were bounded by the surface and core, respectively, with both ending at the $0.5 \times M$ point. Using this initial guess, the results were unconverged, as

seen in Figure 1, so the minimization routine outlined in Section 3 was used to provide the new guess for the final integration. The minimization routine provided a converged result in 65 iterations.

Pc	$1.6257 * 10^{17}\ dyne\ cm^{-1}$
R	$9.9616 * 10^{10}\ cm$
L	$6.2766 * 10^{33}\ erg\ s^{-1}$
Tc	$1.5376 * 10^{7}\ K$

Table 2. Optimized Integration Guesses

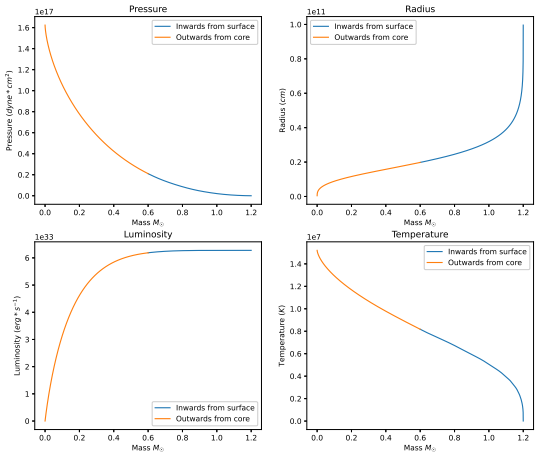

Figure 2. Integrations With Optimized Guess

5. MODEL COMPARISON AND DISCUSSION

After computing the converged model, a comparison was done between this simplistic model and the industry standard stellar interior modeler, MESA (B. Paxton et al. 2011). This model did not do very well at reproducing the results of the MESA model the 1.2 $M_\odot$ star, with most of the surface values having more than a 30 percent difference. This is mainly driven by the radius, which is noticeably higher in the converged result than in either the unconverged case or the MESA result, which extrapolates to a large difference between the surface gravities. This is caused by the minimizer inflating the radius in order to make the pressure and temperature converge.

The luminosity also exhibits large differences, with my model producing a lower value than MESA. The main difference in the luminosity arises from how the pp chain fusion rates are calculated. In my model, I applied a simple $\psi = 1.2$, when in reality it should range from 1 to 1.5 in a star with a helium fraction Y = 0.28. As the pp-chain reactions will dominate the energy generation of this star, the exact rates are important for obtaining the correct luminosity.

Model	L $(erg\ s^{-1})$	R (cm)	$T_{\rm eff}$ (K)	log$g$
This work	$8.263 * 10^{33}$	$1.063 * 10^{11}$	5659	4.149
MESA	$1.284 * 10^{34}$	$7.990 * 10^{10}$	6170	4.397
% Difference	35.7	33.1	8.27	43.5

Table 3. Final values and difference

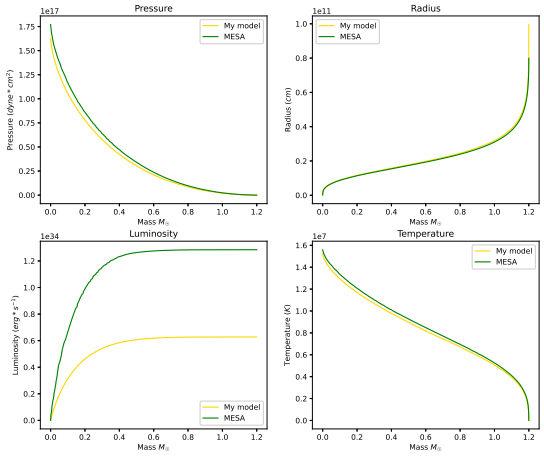

Figure 3. MESA Model Comparison

6. CONCLUSION

I made an attempt at an elementary calculation to determine the properties of a ZAMS star. While the internal structure was well modeled, the surface conditions leave much to be desired, and as such this model may not match well to actual observations of stars.

Software: scipy (P. Virtanen et al. 2020), numpy (C. R. Harris et al. 2020), pandas (T. pandas development team 2020), matplotlib (J. D. Hunter 2007), MESA (B. Paxton et al. 2011),

REFERENCES

Asplund, M., Grevesse, N., & Sauval, A. J. 2005, in Astronomical Society of the Pacific Conference Series, Vol. 336, Cosmic Abundances as Records of Stellar Evolution and Nucleosynthesis, ed. T. G. Barnes, III & F. N. Bash, 25

Byrd, R. H., Lu, P., Nocedal, J., & Zhu, C. 1995, SIAM Journal on Scientific Computing, 16, 1190, doi: 10.1137/0916069

Dormand, J., & Prince, P. 1980, Journal of Computational and Applied Mathematics, 6, 19, doi: https://doi.org/10.1016/0771-050X(80)90013-3

Eddington, A. S. 1920, The Scientific Monthly, 11, 297. http://www.jstor.org/stable/6491

Hansen, C. J., Kawaler, S. D., & Trimble, V. 2004, Stellar interiors : physical principles, structure, and evolution (Springer Science+Business Media New York)

Harris, C. R., Millman, K. J., van der Walt, S. J., et al. 2020, Nature, 585, 357, doi: 10.1038/s41586-020-2649-2

Hunter, J. D. 2007, Computing in Science & Engineering, 9, 90, doi: 10.1109/MCSE.2007.55

Kippenhahn, R., Weigert, A., & Weiss, A. 2012, Stellar Structure and Evolution, Second Edition (Springer-Verlag Berlin Heidelberg)

pandas development team, T. 2020, doi: 10.5281/zenodo.3509134

Paxton, B., Bildsten, L., Dotter, A., et al. 2011, ApJS, 192, 3, doi: 10.1088/0067-0049/192/1/3

Press, W. H., Teukolsky, S. A., Vetterling, W. T., & Flannery, B. P. 2007, Numerical Recipes 3rd Edition: The Art of Scientific Computing, 3rd edn. (USA: Cambridge University Press)

Virtanen, P., Gommers, R., Oliphant, T. E., et al. 2020, Nature Methods, 17, 261, doi: 10.1038/s41592-019-0686-2